

Study of tyrosine and dopa enantiomers as tyrosinase substrates initiating L- and D-melanogenesis pathways

Pedro J. Fernandez-Julia¹
 Jose Tudela-Serrano²
 Francisco Garcia-Molina²
 Francisco Garcia-Canovas²
 Antonia Garcia-Jimenez ²
 Jose L. Munoz-Munoz^{1*}

¹Microbial Enzymology Group, Department of Applied Sciences, Northumberland Building, University of Northumbria, Newcastle Upon Tyne, UK

²GENZ-Group of Research on Enzymology, Department of Biochemistry and Molecular Biology-A, Regional Campus of International Excellence "Campus Mare Nostrum", University of Murcia, Espinardo, Murcia, Spain

Abstract

Tyrosinase starts melanogenesis and determines its course, catalyzing the oxidation by molecular oxygen of tyrosine to dopa, and that of dopa to dopaquinone. Then, nonenzymatic coupling reactions lead to dopachrome, which evolves toward melanin. Recently, it has been reported that D-tyrosine acts as tyrosinase inhibitor and depigmenting agent. The action of tyrosinase on the enantiomers of tyrosine (L-tyrosine and D-tyrosine) and dopa (L-dopa and D-dopa) was studied for the first time focusing on quantitative transient phase kinetics. Post-steady-state transient phase studies revealed that L-dopachrome is formed more rapidly than D-dopachrome. This is due to the lower values of Michaelis constants for L-enantiomers than for D-enantiomers, although the maximum rates are equal for both enantiomers. A deeper analysis of the inter-steady-state transient phase of monophenols

demonstrated that the enantiomer D-tyrosine causes a longer lag period and a lower steady-state rate, than L-tyrosine at the same concentration. Therefore, D-melanogenesis from D-tyrosine occurs more slowly than does L-melanogenesis from L-tyrosine, which suggests the apparent inhibition of melanin biosynthesis by D-tyrosine. As conclusion, D-tyrosine acts as a real substrate of tyrosinase, with low catalytic efficiency and, therefore, delays the formation of D-melanin.

© 2020 The Authors. *Biotechnology and Applied Biochemistry* published by Wiley Periodicals, Inc. on behalf of International Union of Biochemistry and Molecular Biology Volume 68, Number 4, Pages 823–831, 2021

This is an open access article under the terms of the Creative Commons Attribution License, which permits use, distribution and reproduction in any medium, provided the original work is properly cited.

Keywords: tyrosinase, dopa, tyrosine, melanogenesis, lag phase

1. Introduction

Tyrosinase (monophenol, *o*-diphenol: oxygen oxidoreductase, EC 1.14.18.1.) is a copper enzyme that is widely distributed among microorganisms, plants, and animals, in which it shows great similarity between different species [1,2]. It mainly catalyzes two types of reactions: the hydroxylation of monophenols to *o*-diphenols and the oxidation of these *o*-diphenols to their

corresponding *o*-quinones. Both reactions use molecular oxygen as oxidant substrate [3,4]. The monophenolase activity of tyrosinase is the rate-limiting step in the melanin biosynthesis pathway (Fig. S1A).

Several works have studied the stereoselectivity of different tyrosinases [5–8], but no complete kinetic study has been made of the steady-state and transient phase of this process. Steady-state studies of tyrosinase carried out several years ago indicated that the active site of the enzyme had some degree of stereoselectivity [5]. Research with the enzyme obtained from hamster melanoma indicated that the V_{\max} values were the same for the stereoisomers L- and D-tyrosine and L- and D-dopa. However, the K_M values were higher for the D-isomers [6]. Tyrosinase purified from human melanoma cells showed a higher K_M for the D-dopa enantiomer (3 mM) than for the L-dopa enantiomer (0.5 mM) [7]. Although the participation of D-tyrosine in melanogenesis has been studied, there have been few reports on the subject [8].

*Address for correspondence: Jose L. Munoz-Munoz, PhD, FHEA, Microbial Enzymology Group, Department of Applied Sciences, Northumberland Building, University of Northumbria, Newcastle-upon-Tyne NE1 8ST, UK. Tel.: Fax: ; e-mail: jose.munoz@northumbria.ac.uk.

Additional supporting information may be found online in the Supporting Information section at the end of the article.

Received 15 April 2020; accepted 28 July 2020

DOI: 10.1002/bab.1998

Published online 18 August 2020 in Wiley Online Library

(wileyonlinelibrary.com)

As melanoma tyrosinase VH 421 cells showed less affinity for D-dopa than for L-dopa, it was proposed that D-dopa should be added as a cofactor in L-tyrosine assays [9]. Stereoselectivity has also been described in a tyrosinase resistant to organic solvents of *Streptomyces sp.* [10]. Moreover, mutations in the tyrosinase gene of *Ralstonia solanacearum* led to an increase in the k_{cat} for D-tyrosine [11]. Mushroom tyrosinase also showed stereoselectivity when acting on betaxanthins [12]. Using the enzyme from avocado, the same value for V_{max} was described for L-tyrosine and D-tyrosine [13], and the same pattern was obtained for tyrosinase from *Vibrio tyrosinaticus* [14], but not for tyrosinase from *Pseudomonas sp.* [15]. Studies with tyrosinase from *Bacillus megaterium* acting on dopa reveal that ($K_M^D > K_M^L$) in aqueous and organic solvents, for the wild-type [16] and the R209H [17] and V218F [18] mutants.

In addition, it was demonstrated that the inactivation of tyrosinase in its action on L-dopa and D-dopa is also stereoselective, the enzyme showing stereoselectivity in the substrate binding ($K_M^D > K_M^L$), but not in the suicide inactivation constant [19]. A similar event occurred in the inactivation of tyrosinase acting on L- and D-ascorbic acid as the enzyme showed greater affinity for L-ascorbic, although the maximum inactivation rate was the same [20]. Recently, D-tyrosine has been described as a regulator of melanin biosynthesis through the competitive inhibition of tyrosinase activity and the amino acid has been proposed as a possible new skin whitening agent [21].

Enantioselectivity studies of tyrosinase from the creosote bush (*Larrea tridentata*) led to the suggestion that polyphenol oxidase hydroxylates only to the (+) larreatricin form [22]. However, it has recently been shown that this enzyme acts on the two isomers: (-) larreatricin and (+) larreatricin [23]. As regards the kinetics, the values obtained for K_M and k_{cat} do not show the same relationship with the values from NMR experiments, as occurs in the action of mushroom tyrosinase on L-tyrosine and D-tyrosine and L-dopa and D-dopa [24]. As discussed previously [24], the enzyme has greater affinity (lower K_M) for the L forms. However, the V_{max} are the same for both stereoisomers because this parameter depends on the nucleophilic potency of the oxygen of the phenolic hydroxyl, and the NMR of the stereoisomers is the same for the carbon that supports the hydroxyl group. The NMR for larreatricin is described in the Supplementary Material of Ref. [23] and the chemical shift values, δ , are the same for positions 4 and 4' (157.01 ppm), which are the carbons bearing the hydroxyl and which are similar to carbon C-4 of L-tyrosine and D-tyrosine (158.88 and 158.89 ppm, respectively) [24]. The authors of Ref. [23] tested four enzymes: larreatricin hydroxylase from *L. tridentata* (LtPPO), apple tyrosinase (MdPPO1), the fungal tyrosinase from *Agaricus bisporus* (AbPPO4), and the proteolytically activated form of the same (AbPPO4-act). The data shown in Table 1 of Ref. [23] do not correspond to those described in Ref. [24] perhaps because the insolubility of the substrate (larreatricin), the presence of SDS, and the presence of methanol make the measurements difficult to compare. On

Highlights

- The action of tyrosinase on the enantiomers of tyrosine (L-tyrosine and D-tyrosine) and dopa (L-dopa and D-dopa) was studied for the first time focusing on quantitative transient phase kinetics.
- Post-steady-state transient phase studies revealed that L-dopachrome is formed more rapidly than D-dopachrome, due to the lower values of Michaelis constants for L-enantiomers than for D-enantiomers, although the maximum rates are equal for both enantiomers.
- Enantiomer D-tyrosine causes a longer lag period, and a lower steady-state rate, than L-tyrosine at the same concentration. Therefore, D-melanogenesis from D-tyrosine occurs more slowly than does L-melanogenesis from L-tyrosine.

the other hand, it has been reported that human tyrosinase do not oxidize D-tyrosine, that mushroom tyrosinase is not stereoselective on R- and S-rhododendrol, and that human tyrosinase is more efficient on R-rhododendrol [25].

The availability of a highly sensitive method for measuring monophenolase and diphenolase activities [26,27] enabled the stereoselectivity of mushroom, pear, and strawberry tyrosinase to be studied in the steady state [24,28,29]. However, in the present paper, we study, for the first time, L-melanogenesis and D-melanogenesis in the formation of L-dopachrome and D-dopachrome, respectively, from the approaches of the inter-steady-state transient phase for monophenols and post-steady-state transient phase for monophenols and diphenols. The kinetic study should help clarify the recent controversy regarding the role of D-tyrosine in melanogenesis and the methodology for kinetic characterization of the stereoselectivity of tyrosinases.

2. Materials and Methods

2.1. Materials

Mushroom tyrosinase (2,687 U/mg) was purchased from Sigma (Madrid, Spain) and purified as described previously [30]. Bradford's method was used to determine the protein content using bovine serum albumin as standard [31].

L-Tyrosine, L-dopa, D-tyrosine, and D-dopa (Fig. S1B) were obtained from Sigma. Stock solutions of these compounds were prepared in 0.15 mM phosphoric acid to prevent autooxidation. Milli-Q system (Millipore Corp, Billerica, MA) ultrapure water was used throughout.

2.2. Methods

Enzyme activity assay. The enzymatic activity was determined by spectrophotometric techniques using Perkin-Lambda-35 spectrophotometer interconnected online to a computer, in which the kinetic data were recorded, stored, and subsequently

TABLE 1

Parameters and kinetic constants characterizing the action of tyrosinase on tyrosine and dopa enantiomers L and D and their respective δ values for C-3 and C-4

Substrate	Steady-state constants			¹³ C-NMR	
	K_M (mM)	k_{cat} (s ⁻¹)	R	δ_3 (ppm)	δ_4 (ppm)
L-Dopa	0.41 ± 0.04	106.77 ± 2.74		146.92	146.05
D-Dopa	2.11 ± 0.22	108.44 ± 4.08		146.92	146.06
L-Tyrosine	0.31 ± 0.05	8.71 ± 0.89	0.025 ± 0.0004	–	155.88
D-Tyrosine	2.50 ± 0.21	8.71 ± 0.89	0.0075 ± 0.0003	–	155.89

analyzed. All assays were performed in 30 mM phosphate buffer pH 7.0 and at a temperature of 25 °C. The saturating oxygen concentration was 0.26 mM [32–34]. The tests were carried out in triplicate.

Steady-state assays: diphenolase activity on L-dopa and D-dopa. The steady-state rates of tyrosinase in its action on L- and D-dopa were obtained by measuring the dopachrome formation over time at 475 nm [35]. The experimental conditions are detailed in the figure caption.

Post-steady-state assays: diphenolase activity on L-dopa and D-dopa. The absorbance variation over time was followed at 475 nm, with high enzyme (95 nM) and low substrate concentrations (10 μM) ($[D]_0 \ll K_m^D, K_m^L$). These conditions provide a first-order kinetic behavior with respect to the substrate. The enzymatic system evolved in the post-steady-state transient phase until the substrate was fully consumed. This type of transient phase is similar to that seen during active enzyme depletion, in the irreversible inhibition [36] or suicide inactivation of enzymes [37].

Steady-state assays: monophenolase activity of tyrosinase on L-tyrosine and D-tyrosine with o-diphenol (L-dopa or D-dopa) added at $t \rightarrow 0$. Steady-state rates for the action of tyrosinase acting on L- and D-tyrosine were obtained by measuring the dopachrome formation over the time at 475 nm. A lag period was avoided by adding the necessary quantity of o-diphenol to reach the steady-state, $[D]_{ss}$, before adding the enzyme to begin the enzymatic reaction [35]. $[D]_{ss} = R [M]_0$, where $R = 0.042$ in the conditions used in the reaction [35]. In this way, the steady-state phase was reached at the beginning of the reaction, $t \rightarrow 0$.

Post-steady-state transient phase: monophenolase activity of tyrosinase on L-tyrosine and D-tyrosine. The variation of absorbance over time was measured at 475 nm. Having a high enzyme concentration (305 nM) and low substrate concentration (20 nM) ($[M]_0 \ll K_m^D, K_m^L$), first-order kinetic behavior with respect to the substrate was induced [36,37], in the same way as the diphenolase activity (section *Post-Steady-State Assays: Diphenolase Activity on L-Dopa and D-Dopa*).

Inter-steady-state transient phase: monophenolase activity of tyrosinase on L-tyrosine and D-tyrosine with no addition

of o-diphenol (L-dopa or D-dopa) at $t \rightarrow 0$. Enzyme activity was measured at 475 nm, and the formation of dopachrome, without adding o-diphenol before the enzymatic reaction begins, was followed. The concentration of enzyme was 20 nM. The recording pointed to a lag period (τ) between the initial ($t \rightarrow 0$) and final steady-states, during which o-diphenol was accumulated in the medium until it reached $[D]_{ss} = R [M]_0$ in the final steady state [38]. Such an inter-steady-state phase is also characteristic during the slow inhibition of enzymes in the presence of substrate [39].

Kinetic data analysis. Steady-state rate values (V_{ss}) were calculated at different substrate concentrations and then represented *versus* $[D]_0$ or $[M]_0$. These values were fitted to the Michaelis–Menten equation through the Sigma Plot program for Windows [40], which provided the maximum rate (V_{max}) and the apparent Michaelis constant (K_{app}). The REFERASS computer program was used to obtain the rate equations of these mechanisms [41], as detailed in the Appendix of the Supplementary Material (Eqs. A1–A14). Some results of the corresponding experimental procedure can be seen in the figures of the Supplementary Material (Figs. S1 and S2).

NMR assays. The ¹³C-NMR spectra of the L-tyrosine, D-tyrosine, L-dopa, and D-dopa considered here were obtained in a Varian Unity spectrometer of 300 MHz [24,42]. The electronic density of a carbon atom is correlated with the value of its chemical displacement (δ) in ¹³C-NMR [43,44]. Moreover, the nucleophilic power or electron-donating capacity of the oxygen atom of one phenolic hydroxyl has been seen to be inversely correlated with the δ value obtained in ¹³C-NMR in the case of the carbon atom that binds to the hydroxyl group [45].

3. Results and Discussion

In previous studies of the steady-state kinetics of tyrosinase, it was shown that tyrosinase has greater affinity for the L-isomers than for the D-isomers, that is, the Michaelis constant (K_M) was lower for L-enantiomers. However, the maximum rates (V_{max}) were the same for both isomers. These data agree with the values from NMR experiments, since the electron density of the carbons that support the phenolic hydroxyls is identical for the L- and D-isomers (δ_3 and δ_4 are equal), and

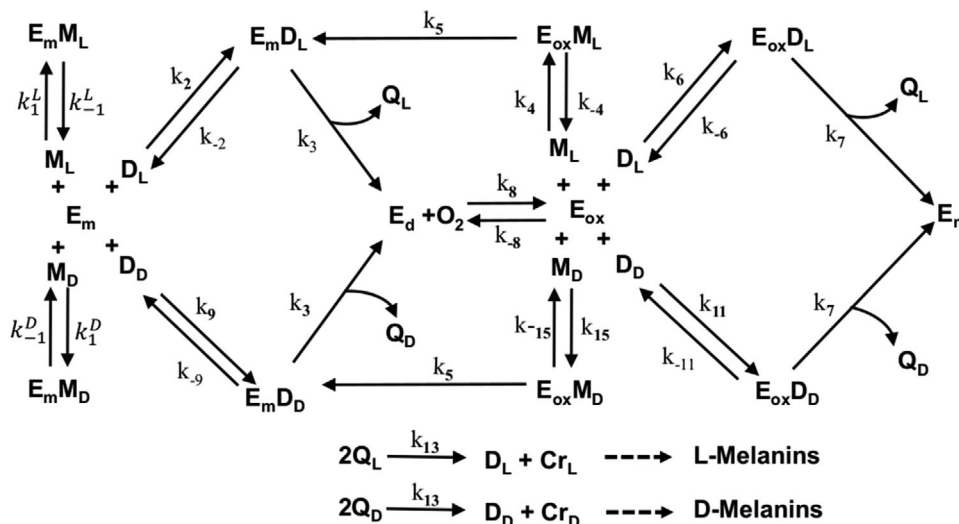


FIG. 1 Mechanism proposed for monophenolase and diphenolase (with $[M] = 0$) activities of tyrosinase, acting on the enantiomers L-tyrosine ($M_L M_L$), D-tyrosine ($M_D M_D$), L-dopa ($D_L D_L$), and D-dopa ($D_D D_D$). Also represented is the formation of the products L-dopachrome (Cr_L), D-dopachrome (Cr_D), L-dopaquinone ($Q_L Q_L$), and D-dopaquinone ($Q_D Q_D$).

thus the nucleophilicity of the oxygens is the same and the nucleophilic attack determines the rate [24,28,29]. However, the time dependence of melanogenesis differs between the L- and D-isomers of tyrosine and is not well explained in the literature where the conclusions are occasionally erroneous [24], as it is shown in Fig. 1 of Ref. [24]. The spectrophotometric recordings for the product generation with time in this figure did not achieve the real steady state in short period times due to the enzyme concentration added to the reaction was low. Because of that, apparently, the lag period for D-tyrosine was shorter than L-tyrosine. This situation can be avoided adding higher enzyme concentrations to the assays reaching the steady state in shorter periods as is presented in this paper (see below) [24].

3.1. Steady-state studies

In these steady-state tests, the accumulation of product *versus* time was measured in such a way that the amount of substrate remained practically constant, since the measurements were made at short times.

Experimental results of diphenolase activity. The action of tyrosinase on L-dopa and D-dopa showed hyperbolic behavior (Figs. S2A and inset.). Analysis of the data by means of nonlinear regression according to the Michaelis equation (Eq. A2) provided the corresponding values of K_M^L , V_{max}^L , V_{max}^D ($V_{max}^L = k_{cat}^L [E]_0 V_{max}^L = k_{cat}^L [E]_0$), K_M^D , and V_{max}^D , V_{max}^D ($V_{max}^D = k_{cat}^D [E]_0 V_{max}^D = k_{cat}^D [E]_0$). These data agree with the values from NMR experiments (Table 1) and the previously published results [24].

To explain the results shown in Table 1, we propose a kinetic mechanism (Fig. 1), in which there are no M or M-enzyme intermediates.

Experimental results of monophenolase activity. It is known that tyrosinase can act on both stereoisomers of monophenols (Fig. S1B), such as L-tyrosine and D-tyrosine [24,28,29]. In the monophenolase activity of tyrosinase, the spectrophotometric recording of the absorbance with respect to time at 475 nm shows a lag period (Fig. 2) [46]. The lag period is the time taken by the enzyme, acting on L-tyrosine or D-tyrosine, to accumulate a certain amount of o-diphenol in the steady-state ($[D]_{ss}[D]_{ss}$) [47]. In our study, the amount of $[D]_{ss}[D]_{ss}$ differed according to whether the L- or D-isomer was being studied, and always must fulfil Eq. (1):

$$R = \frac{[D]_{ss}}{[M]_{ss}} R = \frac{[D]_{ss}}{[M]_{ss}} \quad (1)$$

where $[D]_{ss}[D]_{ss}$ and $[M]_{ss}[M]_{ss}$ represent the concentrations of o-diphenol and monophenol in the steady state. The o-diphenol originates from the evolution of o-dopaquinone to dopachrome [47,48].

For L-isomer:

$$R_L = \frac{[D_L]_{ss}}{[M_L]_{ss}} = \frac{1}{2} \frac{k_5 (k_{-6} + k_7) k_4}{k_7 (k_{-4} + k_5) k_6} \quad (2)$$

For D-isomer:

$$R_D = \frac{[D_D]_{ss}}{[M_D]_{ss}} = \frac{1}{2} \frac{k_5 (k_{-11} + k_7) k_{15}}{k_7 (k_{-15} + k_5) k_{11}} \quad (3)$$

The values of R_L and R_D were determined as indicated in Fig. 2. In the steady state, the excess of accumulated o-diphenol is oxidized by periodate, and is converted into dopachrome, and the value of $[D_L]_{ss}$ or $[D_D]_{ss}$ is calculated from the increase in absorbance at 475 nm taking into account the respective molar absorptivities (Fig. 2) [35,48]. These data facilitate the study of monophenolase activity because it is possible to add to each monophenol concentration the quantity of o-diphenol

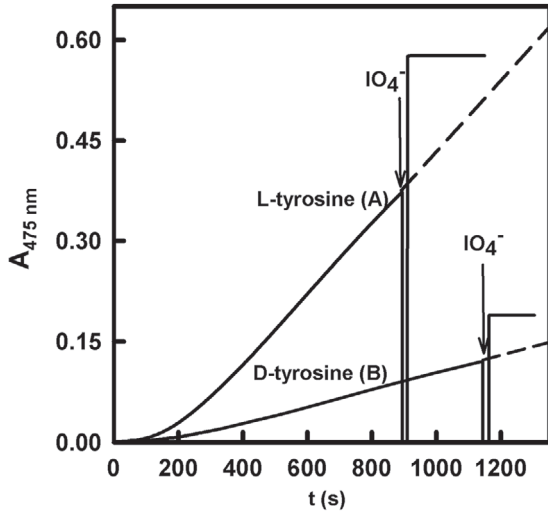


FIG. 2

Spectrophotometric recordings of dopachrome accumulation with time after the action of tyrosinase on tyrosine and assessment of the *o*-diphenol accumulated in the steady-state phase. Curve A: action of tyrosinase on L-tyrosine. The enzyme concentration was 20 nM. The substrate concentration was 0.75 mM. Sodium periodate (NaIO_4) was added in excess at the times indicated in the figure, and the *o*-diphenol present was calculated from the increase in absorbance at 475 nm. Curve B: action of tyrosinase on D-tyrosine. The experimental conditions are the same as in curve A.

corresponding to the steady state ($[D]_{ss}$) [Eq. (1)] at $t = 0$ and so the steady state is reached immediately. The values of the dimensionless parameter R are shown in Table 1.

The experimental results for the steady-state rates in the action of tyrosinase on monophenols are shown in Fig. S2B for L-tyrosine and in Fig. S2B inset for D-tyrosine. In the case of L-tyrosine, the data can be analyzed according to the Michaelis equation (Eq. A8), which provides the corresponding values of K_M^M and V_{max}^M ($V_{max}^M = k_{cat}^M[E]_0$). Note that in the case of D-tyrosine, the low solubility does not allow saturation of the enzyme in these experimental conditions, and, so we work in the first-order region, determining $V_{max}^{M_D}/K_M^{M_D}$. As the value of $V_{max}^{M_L}$ is known, $K_M^{M_D}$ can be determined because $V_{max}^{M_L} = V_{max}^{M_D}$ [24]. Table 1 shows the results obtained. Note that the difference in K_M^{app} values for the monophenolic stereoisomers is greater than in the case of *o*-diphenolics.

To explain the results shown in Table 1 for monophenols, the kinetic mechanism depicted in Fig. 1 is proposed.

3.2. Studies of post-steady-state transient phase

In these experiments, the enzyme rapidly reaches the steady state at $t \rightarrow 0$ and the substrate concentration varies so that the enzyme is in a post-steady-state transient phase, until the substrate is depleted.

The most straightforward kinetic would be:



where S indicates monophenol (M) or *o*-diphenol (D) and Cr indicates the product of the reaction, dopachrome. The substrate concentration through the action of tyrosinase would evolve as follows:

$$\frac{d[S]}{dt} = -\frac{V_{max}[S]}{K_M + [S]} \approx -\frac{V_{max}}{K_M}[S], \quad [S] \ll K_M \quad (5)$$

and the velocity of dopachrome formation would be:

$$\frac{d[\text{Cr}]}{dt} = \frac{V_{max}[S]}{K_M + [S]} \approx \frac{V_{max}}{K_M}[S], \quad [S] \ll K_M \quad (6)$$

Integrating Eq. (5):

$$\int_{[S]_0}^{[S]} \frac{d[S]}{[S]} = -\frac{V_{max}}{K_M} \int_0^t dt \quad (7)$$

gives Eq. (8):

$$[S] = [S]_0 e^{-\frac{V_{max}}{K_M}t} \quad (8)$$

Integrating Eq. (6), taking into account Eq. (8):

$$\int_{[\text{Cr}]_0}^{[\text{Cr}]} d[\text{Cr}] = [S]_0 \int_0^t \frac{V_{max}}{K_M} e^{-\frac{V_{max}}{K_M}t} dt \quad (9)$$

gives Eq. (10):

$$[\text{Cr}] = [S]_0 \left(1 - e^{-\frac{V_{max}}{K_M}t}\right) = [\text{Cr}]_{\infty} \left(1 - e^{-\frac{V_{max}}{K_M}t}\right) \quad (10)$$

with

$$\lambda = \frac{V_{max}}{K_M} \quad (11)$$

where λ is the catalytic power.

Experimental results of diphenolase activity. Figure 3 shows the experimental recordings for the action of the enzyme on L-dopa (recording A), D-dopa (recording E), and different D/L mixtures (recordings B–D). Analysis of these data, by means of nonlinear regression to Eq. (10), provides the values of $[\text{Cr}]_{\infty}$ and the apparent constant λ . Figure 4 shows the values obtained from λ versus percent of L-dopa. Note that increasing concentrations of L-dopa increases the value of λ , as a result of the decrease in $K_M^{D,app}$. Furthermore, the ratio between $\lambda^{D,L}$ for L-dopa and $\lambda^{D,D}$ for D-dopa is:

$$\frac{\lambda^{D,L}}{\lambda^{D,D}} = \frac{V_{max}^{D,L}/K_M^{D,L}}{V_{max}^{D,D}/K_M^{D,D}} = \frac{K_M^{D,D}}{K_M^{D,L}}, \quad V_{max}^{D,L} \approx V_{max}^{D,D} \quad (12)$$

which agrees with the experimental data (Tables 1 and 2).

Experimental results of monophenolase activity during post-steady-state transient phase. The action of tyrosinase on L-tyrosine, D-tyrosine, and on different mixtures of D and L is shown in Fig. 5. In these experiments, the amount of *o*-diphenol (D or L) corresponding to the ratio R (R_D or R_L) is added at $t \rightarrow 0$. Thus, the system reaches the steady state at $t \rightarrow 0$, and evolves in the post-steady-state transient phase until the

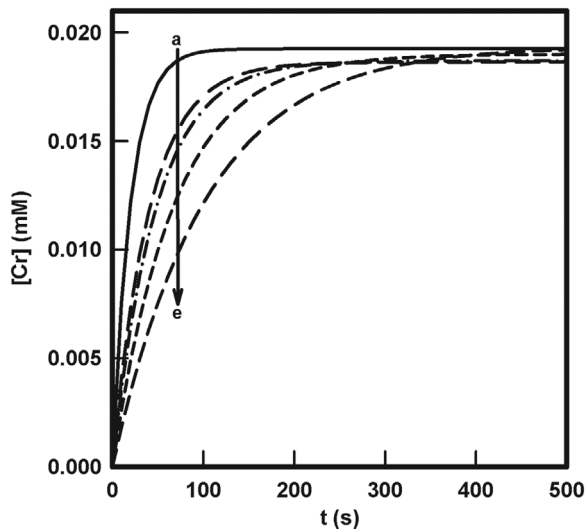


FIG. 3 Post-steady-state transient phase assays of diphenolase activity. Experimental recordings at $\lambda = 475 \text{ nm}$ of dopachrome formation from the consumption of L-dopa (A), D-dopa (E), and mixtures of both acting on the enzyme in a first-order kinetics. The experimental conditions were: (A) 100% L-dopa, (B) 75% L-dopa and 25% D-dopa, (C) 50% L-dopa and 50% D-dopa, (D) 25% of L-dopa and 75% of D-dopa, and (E) 100% of D-dopa.

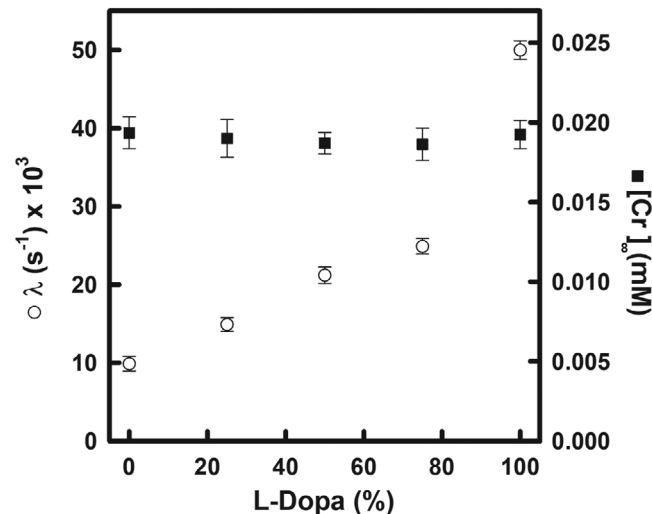


FIG. 4 Post-steady-state transient phase assays of diphenolase activity. Representation of the values of the first-order constant (λ) and the product, dopachrome, obtained at the final reaction time versus the percentage of L-form in the experiment.

substrate is consumed. Analysis by nonlinear regression of the experimental recordings shown in Fig. 5, according to Eq. (10), provide the values of λ and $[\text{Cr}]_{\infty}$ shown in Fig. 6. Note how the value of λ increases with increasing concentrations of the L-form because $K_M^{D,app}$ decreases. In this case, the ratio between $\lambda^{M,L}$ for L-tyrosine and $\lambda^{M,D}$ for D-tyrosine is:

$$\frac{\lambda^{M,L}}{\lambda^{M,D}} = \frac{V_{\max}^{M,L}/K_M^{M,L}}{V_{\max}^{M,D}/K_M^{M,D}} = \frac{K_M^{M,D}}{K_M^{M,L}}, \quad V_{\max}^{M,L} \approx V_{\max}^{M,D} \quad (13)$$

which agrees with the experimental data (Tables 1 and 2).

3.3. Effect of substrate stereoisomerism on the lag period of monophenolase activity of tyrosinase. Study of inter-steady-state transient phase

In its action on monophenols, tyrosinase shows a lag period before it reaches the final steady state. This lag period " τ " is the time necessary to accumulate in the medium a certain concentration of *o*-diphenol in the medium as a result of the

chemical evolution of *o*-dopaquinone [46-48]. This concentration of *o*-diphenol is described by Eq. (1). The analytical expression of the lag period is obtained by applying the balance of matter in the steady-state and gives [46]:

$$\tau = \frac{R(K_M^M + [M_L]_0)}{V_{\max}^{Cr(M_L)}} + \frac{1}{2k_{app}} \quad (14)$$

In this equation, K_M^M is the Michaelis constant for monophenol ($K_M^{M_L}$ or $K_M^{M_D}$, respectively), $[M]_0$ is the concentration of monophenol ($[M_L]_0$ or $[M_D]_0$) and $V_{\max}^{Cr(M)}$ is the maximum rate expressed in the formation of dopachrome (Cr). Finally, k_{app} is the apparent constant of transformation of *o*-dopaquinone into dopachrome.

For each of the isomers, the expression of the lag period takes the form of:

$$\tau_L = \frac{R_L(K_M^L + [M_L]_0)}{V_{\max}^{Cr(M_L)}} + \frac{1}{2k_{app}} \quad (15)$$

and

$$\tau_D = \frac{R_D(K_M^D + [M_D]_0)}{V_{\max}^{Cr(M_D)}} + \frac{1}{2k_{app}} \quad (16)$$

TABLE 2

Ratio between Michaelis constants and catalytic powers of the enantiomers of tyrosine and dopa

Steady state		Post-steady-state transient phase	
$K_M^{D-dopa} / K_M^{L-dopa}$	$K_M^{D-dopa} / K_M^{L-dopa}$	$\lambda^{L-dopa} / \lambda^{D-dopa}$	$\lambda^{L-dopa} / \lambda^{D-dopa}$
	5.14 ± 0.73		5.1 ± 0.21
$K_M^{D-tyrosine} / K_M^{L-tyrosine}$		$\lambda^{L-tyrosine} / \lambda^{D-tyrosine}$	$\lambda^{L-tyrosine} / \lambda^{D-tyrosine}$
	8.06 ± 1.48		8.07 ± 0.17

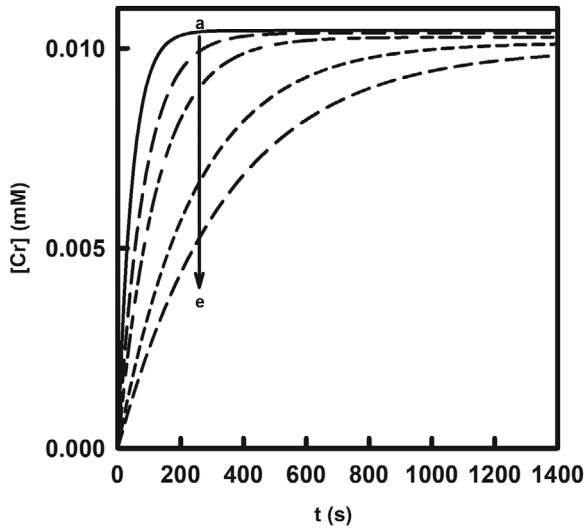


FIG. 5

Post-steady-state transient phase assays of monophenolase activity. Experimental recordings of the accumulation of dopachrome from the consumption of L-tyrosine and D-tyrosine and their mixtures acting the enzyme in a first-order kinetics. The experimental conditions were: (A) 100% L-tyrosine, (B) 75% L-tyrosine and 25% D-tyrosine, (C) 50% L-tyrosine and 50% D-tyrosine, (D) 25% L-tyrosine and 75% D-tyrosine, and (E) 100% D-tyrosine. L-Dopa or D-dopa was added to attain the ratios $R_L = [D_L]/[M_L]$, $R_D = [D_D]/[M_D]$ and $R_D = [D_D]/[M_D]$.

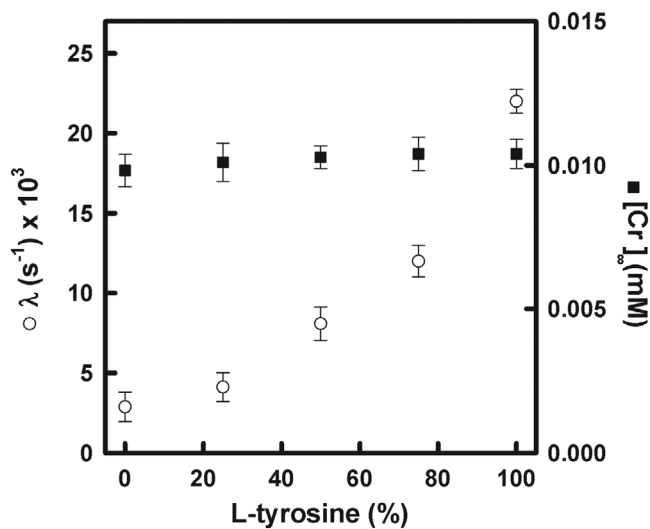


FIG. 6

Post-steady-state transient phase assays of monophenolase activity. Representation of the values of the apparent first-order constant (λ) and the concentration of product, dopachrome, accumulated at the final reaction time ($[Cr]_{\infty}$). Values obtained in the action of tyrosinase on L and D-tyrosine versus the proportion of L-tyrosine in the assay, from experimental recordings of Fig. 2 fitted to Eq. 10.

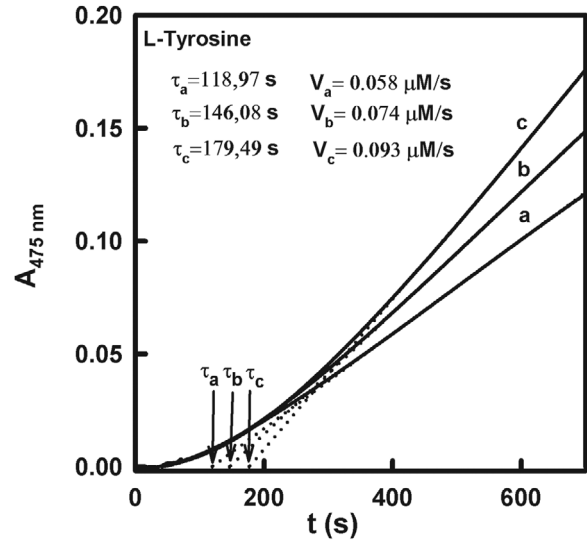


FIG. 7

Inter-steady-state transient phase assays of monophenolase activity. Curves of accumulation of dopachrome in the action of tyrosinase on L-tyrosine, varying the substrate concentration. The concentrations of L-tyrosine were (mM): (A) 0.2, (B) 0.4, and (C) 0.75. The figure shows the values of τ and their graphic representation.

The equation rate in the steady state is:

$$V_{ss}^{Cr(M_L)} = \frac{V_{max}^{Cr} [M_L]_0}{K_M^{M_L} + [M_L]_0} \quad (17)$$

and

$$V_{ss}^{Cr(M_D)} = \frac{V_{max}^{Cr} [M_D]_0}{K_M^{M_D} + [M_D]_0} \quad (18)$$

As $K_M^{M_D} > K_M^{M_L}$ (Table 1), for the same monophenol concentration:

$$V_{ss}^{Cr(M_D)} < V_{ss}^{Cr(M_L)} \quad (19)$$

Furthermore, the equation for the lag phase, [Eqs. (15) and (16)], gives:

$$R_D (K_M^D + [M_D]_0) > R_L (K_M^L + [M_L]_0) \quad (20)$$

Consequently, according to Eqs. (15) and (16), the lag period is greater for isomer D- than for L-, which means that in the qualitative study published by our group previously, the enzymatic reactions had not reached the steady-state.[24]

Inter-steady-state transient phase of the monophenolase activity without addition of o-diphenol at $t \rightarrow 0$: experimental results. The assays of monophenolase activity of tyrosinase acting on L- or D-tyrosine show a lag period that lasts until the system reaches the final steady state (Eqs. 15 and 16). This lag period increases when the substrate concentration increases, as shown in Fig. 7 for the L-isomer. Similar behavior was observed for the D-isomer but, in this case, the lag periods were longer and the steady-state rate was lower (Fig. 8).

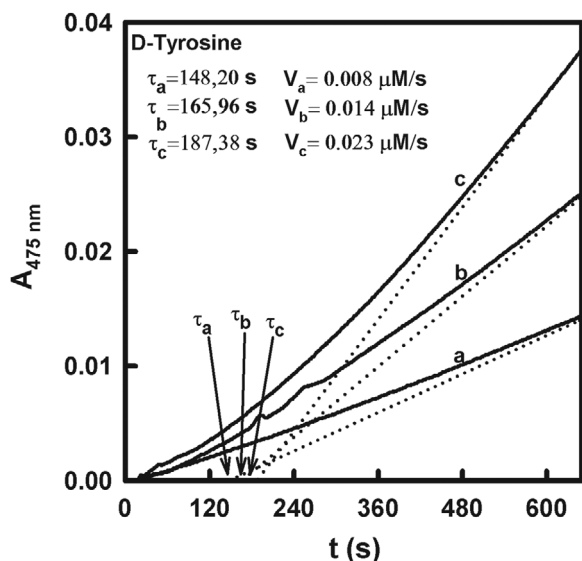


FIG. 8

Inter-steady-state transient phase assays of monophenolase activity. Dopachrome accumulation curves in the action of tyrosinase on D-tyrosine, varying the substrate concentration. The substrate concentrations were (mM): (A) 0.2, (B) 0.4, and (C) 0.75. In the figure, the values of τ and their graphic representation are indicated.

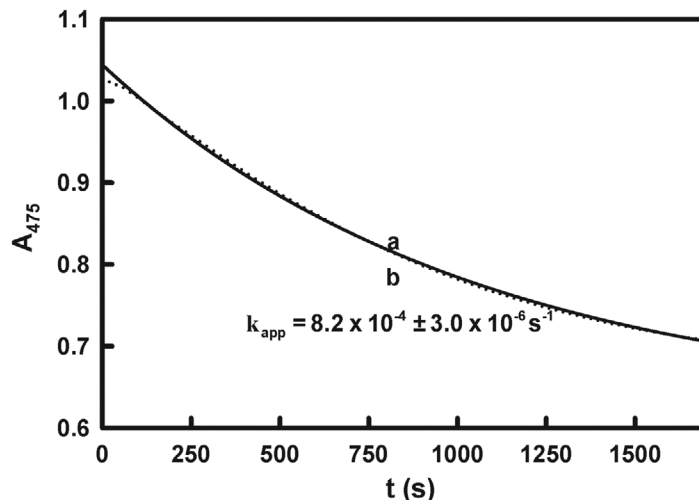


FIG. 9

Chemical evolution of D and L-dopachrome. The reaction medium was: (A) L-dopa (1.5 mM) and NaIO₄ (0.2 mM) and (B) D-dopa (1.5 mM) and NaIO₄ (0.2 mM). The evolution of absorbance with time was recorded. The value of the apparent rate constant was obtained from an analysis of the recordings according to a first order kinetics.

A comparison of the experiments involving the L- and D-tyrosine forms using the low and same concentration of enzyme, as well as the same concentration of substrate, shows that the amount of dopachrome that leads to a given amount of melanin in a given time is much lower in the case of the D-isomers [21,25]. This would explain (Eqs. 15, 16, and 20) why the D-tyrosine form is sometimes not considered as a tyrosinase substrate [21,25].

In this work, dopachrome is considered to be the final product of the proximal phase of melanogenesis. However, dopachrome is not completely stable, but evolves into melanin, and the same occurs with dopaminochrome [48-50], during the distal phase of melanogenesis. As can be seen in Fig. 9, the chemical evolution of L-dopachrome and D-dopachrome shows the same kinetics. Therefore, the only difference lies in the proximal phase of melanogenesis because the formation of D-dopachrome from D-tyrosine is slower than L-dopachrome production from L-tyrosine.

Recently, the study of tyrosinase stereoselectivity has grown in importance due to: (i) its reactivity toward D and L-tyrosine, its physiological substrate [21]; (ii) the action of human tyrosinase on rhododendrol, which induces leukoderma [25]; and (iii) the origin of antiviral and anticancer properties of creosote bush lignans *in vivo*, which has also been studied, considering the action of polyphenol oxidase on (+) and (-) larreatricin.[22,23]

It has been proposed that D-tyrosine negatively regulates melanin biosynthesis by competitively inhibiting tyrosinase

activity in human MNT1 melanoma cells and primary human melanocytes [21]. However, it must be taken into account that these experiments were carried out with the same concentration of substrate (L-tyrosine or D-tyrosine), the same concentration of enzyme and always the same reaction time. According to the data presented in Ref. [21], the effect of D-tyrosine increases the lag period and slows down dopachrome formation. Thus, melanin accumulation is lower from the D-enantiomer than from L-tyrosine when they are compared under the same conditions. In Fig. 3 of Ref. [21], the accumulation of melanin increases as the concentration of D-tyrosine increases (Figs. 3a and 3d). These experiments indicate that D-tyrosine competes with L-tyrosine for the active site of the enzyme, but acts as a competitive substrate that generates the same product (*o*-dopaquinone → dopachrome) [48,49]. This means that D-tyrosine cannot be proposed as a new skin-whitening agent.

4. Conclusions

The action of tyrosinase on the stereoisomers of tyrosine and dopa was studied following three experimental kinetic approaches. Our studies of the steady state showed that V_{max}^D and K_m^D are higher than V_{max}^L and K_m^L for both tyrosine and dopa. The study based on the post-steady-state transient phase, provided data which agreed with those obtained for the steady-state approach. However, the results obtained for the inter-steady-state transient phase demonstrate that the lag period is longer and the steady-state rate is slower for D-tyrosine than for L-tyrosine. Thus, D-tyrosine delays D-melanogenesis compared

with L-melanogenesis from L-tyrosine. In the case of D-dopa, the rate of D-dopachrome formation is slower than that of L-dopachrome from L-dopa, but the limiting process is D-tyrosine hydroxylation. Consequently, the above experimental results demonstrate that D-tyrosine is not a true tyrosinase inhibitor and is capable of preventing or significantly decreasing L-melanogenesis. D-Tyrosine is an alternative substrate of tyrosinase that originates D-melanogens and D-melanin, although more slowly than the corresponding biosynthesis of L-melanogens and L-melanin from L-tyrosine.

5. Acknowledgements

J.M.-M. received funding from internal grants in Northumbria University. This work was partially supported by the SAF2016-77241-R project from the Ministerio de Ciencia, Innovacion y Universidades (Madrid, Spain), the 20809/PI/18 and 20961/PI/18 projects from Fundacion Seneca (CARM, Murcia, Spain), and AEIP-15452 project from Murcia University (Murcia, Spain).

6. Conflict of Interest

The authors have no conflict of interest to declare.

7. References

- [1] Kanteev, M., Goldfeder, M., and Fishman, A. (2015) *Protein Sci.* 24, 1360-1369.
- [2] Mann, T., Gerwat, W., Batzer, J., Eggers, K., Scherner, C., Wenck, H., Stab, F., Hearing, V. J., Rohm, K. H., and Kolbe, L. (2018) *J. Invest. Dermatol.* 138, 1601-1608.
- [3] Solomon, E. I. (1996) Sundaram, U. M., and Machonkin, T. E. *Chem. Rev.* 96, 2563-2605.
- [4] Sanchez-Ferrer, A., Rodriguez-Lopez, J. N., Garcia-Canovas, F., and Garcia-Carmona, F. (1995) *Biochim. Biophys. Acta* 1247, 1-11.
- [5] Harrison, W. H., Whisler, W. W., and Ko, S. (1967) *J. Biol. Chem.* 242, 1660-1667.
- [6] Pomerantz, S. H. (1963) *J. Biol. Chem.* 238, 2351-2357.
- [7] Jergil, B., Lindbladh, C., Rorsman, H., and Rosengren, E. (1983) *Acta Derm-Venereol* 63, 468-475.
- [8] Chen, Y. M., and Chavin, W. (1969) *Anal. Biochem.* 27, 463-472.
- [9] Winder, A. J., and Harris, H. (1991) *Eur. J. Biochem.* 198, 317-326.
- [10] Ito, M., and Oda, K. (2000) *Biosci. Biotechnol. Biochem.* 64, 261-267.
- [11] Molloy, S., Nikodinovic-Runic, J., Martin, L. B., Hartmann, H., Solano, F., Decker, H., and O'Connor, K. E. (2013) *Biotechnol. Bioeng.* 110, 1849-1857.
- [12] Gándia-Herrero, F., Escribano, J., and Garcia-Carmona, F. (2005) *J. Agric. Food Chem.* 53, 9207-9212.
- [13] Kahn, V., and Pomerantz, S. H. (1980) *Phytochemistry* 19, 379-385.
- [14] Pomerantz, S. H., and Murthy, V. V. (1974) *Arch. Biochem. Biophys.* 160, 73-82.
- [15] Yoshida, H., Tanaka, Y., and Nakayama, K. (1974) *Agric. Biol. Chem.* 38, 627-632.
- [16] Shuster, V., and Fishman, A. (2009) *J. Mol. Microbiol. Biotechnol.* 17, 188-200.
- [17] Ben-Yosef, V. S., Sendovski, M., and Fishman, A. (2010) *Enzyme Microb. Technol.* 47, 372-376.
- [18] Goldfeder, M., Kanteev, M., Adir, N., and Fishman, A. (2013) *Biochim. Biophys. Acta* 1834, 629-633.
- [19] Munoz-Munoz, J. L., Acosta-Motos, J. R., Garcia-Molina, F., Varon, R., Garcia-Ruiz, P. A., Tudela, J., Garcia-Canovas, F., and Rodriguez-Lopez, J. N. (2010) *Biochim. Biophys. Acta* 1804, 1467-1475.
- [20] Munoz-Munoz, J. L., Garcia-Molina, F., Garcia-Ruiz, P. A., Varon, R., Tudela, J., and Garcia-Canovas, F. (2009) *Biochim. Biophys. Acta* 1794, 244-253.
- [21] Park, J., Jung, H., Kim, K., Lim, K. M., Kim, J. Y., Jho, E. H., and Oh, E. S. (2018) *Pigment Cell Melanoma Res.* 31, 374-383.
- [22] Cho, M. H., Moinuddin, S. G. A., Helms, G. L., Hishiyama, S., Eichinger, D., Davin, L. B., Lewis, N. G. (2003) *Proc. Natl. Acad. Sci. USA* 100, 10641-10646.
- [23] Martin, H. J., Kampatsikas, I., Oost, R., Pretzler, M., Al-Sayed, E., Roller, A., Giester, G., Rompel, A., and Maulide, N. (2018) *Chemistry* 24, 15756-15760.
- [24] Espin, J. C., Garcia-Ruiz, P. A., Tudela, J., and Garcia-Canovas, F. (1998) *Biochem. J.* 331, 547-551.
- [25] Ito, S., Gerwat, W., Kolbe, L., Yamashita, T., Ojika, M., and Wakamatsu, K. (2014) *Pigment Cell Melanoma Res.* 27, 1149-1153.
- [26] Rodriguez-Lopez, J. N., Escribano, J., and Garcia-Canovas, F. (1994) *Anal. Biochem.* 216, 205-212.
- [27] Espin, J. C., Morales, M., Varon, R., Tudela, J., and Garcia-Canovas, F. (1996) *J. Food Sci.* 61, 1177-1182.
- [28] Espin, J. C., Garcia-Ruiz, P. A., Tudela, J., and Garcia-Canovas, F. (1998) *J. Agric. Food Chem.* 46, 2469-2473.
- [29] Marin-Zamora, M. E., Rojas-Melgarejo, F., Garcia-Canovas, F., and Garcia-Ruiz, P. A. (2007) *J. Agric. Food Chem.* 55, 4569-4575.
- [30] Rodriguez-Lopez, J. N., Fenoll, L. G., Garcia-Ruiz, P. A., Varon, R., Tudela, J., Thorneley, R. N. F., and Garcia-Canovas, F. (2000) *Biochemistry* 39, 10497-10506.
- [31] Bradford, M. M. (1976) *Anal. Biochem.* 72, 248-254.
- [32] Rodriguez-Lopez, J. N., Ros, J. R., Varon, R., and Garcia-Canovas, F. (1993) *Biochem. J.* 293, 859-866.
- [33] Fenoll, L. G., Rodriguez-Lopez, J. N., Garcia-Molina, F., Garcia-Canovas, F., and Tudela, J. (2002) *Int. J. Biochem. Cell Biol.* 34, 332-336.
- [34] Garcia-Molina, F., Hiner, A. N. P., Fenoll, L. G., Rodriguez-Lopez, J. N., Garcia-Ruiz, P. A., Garcia-Canovas, F., and Tudela, J. (2005) *J. Agric. Food Chem.* 53, 3702-3709.
- [35] Garcia-Molina, F., Munoz, J. L., Varon, R., Rodriguez-Lopez, J. N., Garcia-Canovas, F., and Tudela, J. (2007) *J. Agric. Food Chem.* 55, 9739-9749.
- [36] Liu, W., and Tsou, C. L. (1986) *Biochim. Biophys. Acta* 870, 185-190.
- [37] Munoz-Munoz, J. L., Garcia-Molina, F., Garcia-Ruiz, P. A., Molina-Alarcon, M., Tudela, J., Garcia-Canovas, F., and Rodriguez-Lopez, J. N. (2008) *Biochem. J.* 416, 431-440.
- [38] Fenoll, L. G., Rodriguez-Lopez, J. N., Garcia-Sevilla, F., Garcia-Ruiz, P. A., Varon, R., Garcia-Canovas, F., and Tudela, J. (2001) *Biochim. Biophys. Acta-Protein Struct. Mol. Enzym.* 1548, 1-22.
- [39] Morrison, J. F. (1982) *Trends Biochem. Sci.* 7, 102-105.
- [40] Jandel-Scientific (2016) Sigma Plot for Windows™, Corte Madera.
- [41] Varon, R., Garcia-Sevilla, F., Garcia-Moreno, M., Garcia-Canovas, F., Peyro, R., and Duggleby, R. G. (1997) *Comp. Appl. Biosci.* 13, 159-167.
- [42] Espin, J. C., Varon, R., Fenoll, L. G., Gilabert, M. A., Garcia-Ruiz, P. A., Tudela, J., and Garcia-Canovas, F. (2000) *Eur. J. Biochem.* 267, 1270-1279.
- [43] Gunther, H., Herrig, W., Seel, H., Tobias, S., Demeijere, A., and Schrader, B. (1980) *J. Org. Chem.* 45, 4329-4333.
- [44] Farnum, D. G., and Wolf, A. D. (1974) *J. Am. Chem. Soc.* 96, 5166-5175.
- [45] Tomiyama, S., Sakai, S., Nishiyama, T., and Yamada, F. (1993) *Bull. Chem. Soc. Jpn.* 66, 299-304.
- [46] Garcia-Molina, F., Munoz, J. L., Varon, R., Rodriguez-Lopez, J. N., Garcia-Canovas, F., and Tudela, J. (2007) *Int. J. Biochem. Cell Biol.* 39, 238-252.
- [47] Ros, J. R., Rodriguez-Lopez, J. N., and Garcia-Canovas, F. (1994) *Biochim. Biophys. Acta* 1204, 33-42.
- [48] Cabanes, J., Garcia-Canovas, F., Lozano, J. A., and Garcia-Carmona, F. (1987) *Biochim. Biophys. Acta* 923, 187-195.
- [49] Garcia-Carmona, F., Garcia-Canovas, F., Iborra, J. L., and Lozano, J. A. (1982) *Biochim. Biophys. Acta* 717, 124-131.
- [50] Garcia-Moreno, M., Rodriguez-Lopez, J. N., Martinez-Ortiz, F., Tudela, J., Varon, R., and Garcia-Canovas, F. (1991) *Arch. Biochem. Biophys.* 288, 427-434.